Localization and Orientation of Functional Water Molecules in Bacteriorhodopsin as Revealed by Polarized Fourier Transform Infrared Spectroscopy

Minoru Hatanaka, Hideki Kandori, and Akio Maeda
Department of Biophysics, Graduate School of Science, Kyoto University, Kyoto 606-01, Japan

ABSTRACT Linear dichroic difference Fourier transform infrared spectra upon formation of the M photointermediate were recorded with oriented purple membranes. The purpose was to determine the angle of the directions of the dipole moments of 1) the water molecule whose O-H stretching vibration appears at 3643 cm^{-1} for the unphotolyzed state and 3671 cm^{-1} for the M intermediate, and 2) the C=O bond of protonated Asp85 in the M intermediate. The angle of 36° we find for the C=O of the protonated Asp85 in the M intermediate is not markedly different from 26° for unprotonated Asp85 in the model based on cryoelectron diffraction, indicating the absence of gross orientation changes in Asp85 upon its protonation. The O-H band at 3671 cm^{-1} of a water molecule in the M intermediate, although its position has not determined, is fixed almost parallel to the membrane plane. For the unphotolyzed state the angle of the water O-H to the membrane normal was determined to be 60°. On the basis of these data and the structural model, we place the water molecule in the unphotolyzed state at a position where it forms hydrogen bonds with the Schiff base, Asp85, Asp212, and Trp86.

INTRODUCTION

Bacteriorhodopsin is one of the membrane proteins in *Halobacterium salinarium* and functions as a proton pump. It has a retinal chromophore covalently bound to Lys^{216} through a Schiff base linkage. Upon photoreaction, a proton moves from the cytoplasmic to the extracellular side via the Schiff base through the membrane. In this process bacteriorhodopsin forms a series of intermediates named K, L, M, N, and O, which are distinguished by their visible absorption spectra. In the L-to-M conversion, the proton is transferred from the Schiff base to Asp^{85}, which is also the counterion of the Schiff base in the L intermediate as well as the unphotolyzed state (see Lanyi, 1993; Maeda et al., 1997; for reviews). The replacement of Asp^{85} by a neutral residue abolishes this reaction. Asp^{85} is also surrounded by the charged residues Asp^{212} and Arg^{82}. These are dispensable, however, for proton pumping because replacement of both Asp^{212} and Arg^{82} does not abolish transport (Brown et al., 1995b).

The structural model of bacteriorhodopsin by electron diffraction at 0.35-nm resolution (Grigorieff et al., 1996) is quite instructive, but its resolution is not sufficient for complete clarification of the structure around the Schiff base, especially for the location of water molecules. Fourier transform infrared (FTIR) spectroscopy for the photointermediates has contributed greatly to the detection of changes in hydrogen bonding at this site (Maeda et al., 1994; Fischer et al., 1994; Kandori et al., 1995; Chon et al., 1996). The difference spectrum upon formation of the M intermediate exhibits a bilobed feature at 3643 (−) and 3671 (+) cm^{-1} (Maeda et al., 1992; Hatanaka et al., 1996). These O-H stretching vibrations could not originate from a symmetrical water molecule in the protein environment. The negative band has been ascribed to the one of the two O-H bonds that weakly H-bonds with Asp^{212}, whereas the other binds strongly with Asp^{85} (Maeda et al., 1994; Kandori et al., 1995). The effect of halides in D85T in place of Asp^{85} is explained by a water molecule between the Schiff base and the counterion (Chon et al., 1996). However, the relationship of this water molecule to the Schiff base has not been sufficiently elucidated. Difference FTIR spectra with a polarized probe beam were shown to be useful for determining the orientation of the various parts of the retinal skeleton and a carboxylic acid in bacteriorhodopsin (Earnest et al., 1986; Fahmy et al., 1989).

The present study aims at determining the orientation of the O-H bonds of water molecules, whose stretching vibration shows a bilobed shape in the FTIR spectrum upon M formation (Maeda et al., 1992; Hatanaka et al., 1996). On the basis of the present results and the structure model by Grigorieff et al. (1996), a plausible geometry of the water molecule in the active site is proposed that accounts for the orientation angle of this water molecule and Asp^{85} in the region close to the Schiff base.

MATERIALS AND METHODS

Purple membranes were prepared by the method described by Oesterhelt and Stoeckenius (1974). The membranes were suspended in 5 mM borate buffer (pH 10), and its 80-μl aliquot was dried in room air on a BaF_2 window with a diameter of 18 mm. After hydration by 1 μl of water, the sample was placed in a cell and then mounted in an Oxford DN-1704 cryostat. The film was illuminated with >500-nm light for 1 min at 273 K to obtain the light-adapted state of bacteriorhodopsin (BR), and cooled

Received for publication 15 January 1997 and in final form 1 May 1997.
Address reprint requests to Dr. Akio Maeda, Department of Biophysics, Graduate School of Science, Kyoto University, Kitashirakawa-oiwake-cho, Sakyo-ku, Kyoto 606-01, Japan. Tel.: 81-75-753-4210; Fax: 81-75-753-4210; E-mail; maeda@photo2.biophys.kyoto-u.ac.jp.

0006-3495/97/08/1001/06 $2.00

after 10 min for complete decay of the N intermediate that was produced under these conditions.

The illumination with >500-nm light at 230 K for 1 min converted BR to the M intermediate. It was quite stable, and no traces of the L intermediate were formed under these conditions. Spectral changes in the visible region under these conditions show the typical spectral changes from 570 nm to 412 nm for the formation of the M intermediate. Any contributions of P_{500} and P_{380} species at alkaline pH (Balashov et al., 1991) were not detected (not shown). Because the M intermediate completely reverted to BR upon illumination with 420-nm light for 3 min, as envisaged by the same spectral shape, these cycles of alternative illuminations with >500-nm light and 420-nm light were repeated three times. The difference spectrum was calculated from the spectra constructed with 128 interferograms before and after the illumination. The six spectra thus obtained were averaged for the M minus BR spectrum. Linear dichroism was measured by mounting a BaF_2 polarizer in the vertical *xy* plane in front of a mercury-cadmium-technetium detector in a Bio-Rad FTS40 FTIR spectrometer. The IR probe light travels along the *z* axis to the window with the vertical and horizontal polarizations, A_V and A_H, in the *xz* and *yz* planes, respectively. The probe light focused on the sample in this instrument can be regarded as an essentially parallel beam. The window in the *xy* plane can be tilted around the vertical *x* axis by rotation of the rod holding the window. The tilt angles (ϕ_0) were 0°, 10.7°, 21.4°, 32.1°, 42.8°, and 53.5°.

The dichroic ratio *R* is defined as

$$R = [A_H(\phi_0)/A_H(0°)]/[A_V(\phi_0)/A_V(0°)] \quad (1)$$

Increases in the effective number of the BR molecules absorbing light with tilting were corrected by increasing the intensity of the A_V component. *R* is related to the angle of the dipole moment to the membrane normal θ_0 by the equation described by Rothschild and Clark (1979),

$$R = 1 + \sin^2\phi_0/n^2 \times [\rho\langle 9\cos^2\theta_0 - 3\rangle]/[2 - \rho\langle 3\cos^2\theta_0 - 1\rangle] \quad (2)$$

where *n*, the refractive index of the film in the IR region, was assumed to be 1.7, as used previously (Earnest et al., 1986), and ρ, the degree of orientation of the membrane, was assumed to be 0.95, as reported by Earnest et al. (1986). The assumption for the latter is rational, as judged from the intensity ratio of amide II/amide I in our unhydrated film of 1.02, in comparison with their value of 0.98.

RESULTS

Fig. 1 shows a series of A_V (*a*) and A_H (*b*) components of the M minus BR spectra in the 1800–1670 cm^{-1} region. The changes were most prominent in the amide I bands in 1700–1670 cm^{-1}. These bands have not yet been assigned to any specific modes, and change in a complex way because of cancellation of positive and negative bands. Hence they were not analyzed further. The positive peak at 1761 cm^{-1} has been assigned to the C=O stretching vibration of protonated Asp^{85} (Braiman et al., 1988), and is almost free from other spectral components. The A_H component of the 1761 cm^{-1} band increases in intensity when the window is tilted. Slight increases in the intensity of the A_V component were used for correction by the tilting, as described in Materials and Methods. The 1761-cm^{-1} band was fitted by a Gaussian function with a constant full width at half-maximum (FWHM), and the *R* value was calculated for each ϕ_0. The *R* versus ϕ_0 plot for this band can be best fitted with a curve of Eq. 2 with $\theta_0 = 36°$ (Fig. 2, *closed circles and the bold line through them*). The results of three independent experiments were averaged. The 1527, 1202, and 1169 cm^{-1} bands of the retinal polyene chain show 72 ± 0.7°, 75 ± 2.3°, and 66 ± 1.3°, respectively (*open circles, closed squares, and closed triangles, respectively, and the*

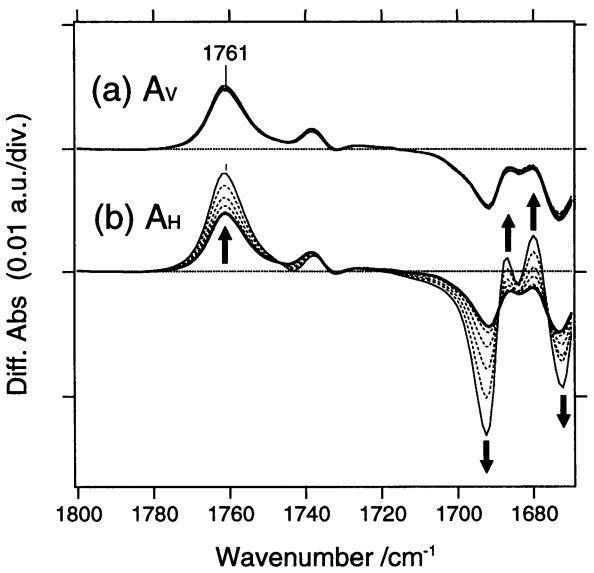

FIGURE 1 Changes of the M minus BR spectra in the 1800–1670 cm^{-1} region with the tilting of the sample window for the A_V (*a*) and A_H (*b*) components. The thick solid lines are the spectra at $\phi_0 = 0°$; the dotted lines are those at $\phi_0 = 10.7$, 21.4, 32.1, and 42.8°; and the solid thin lines are those at $\phi_0 = 53.5°$. Arrows indicate the direction for the spectral changes with the tilting.

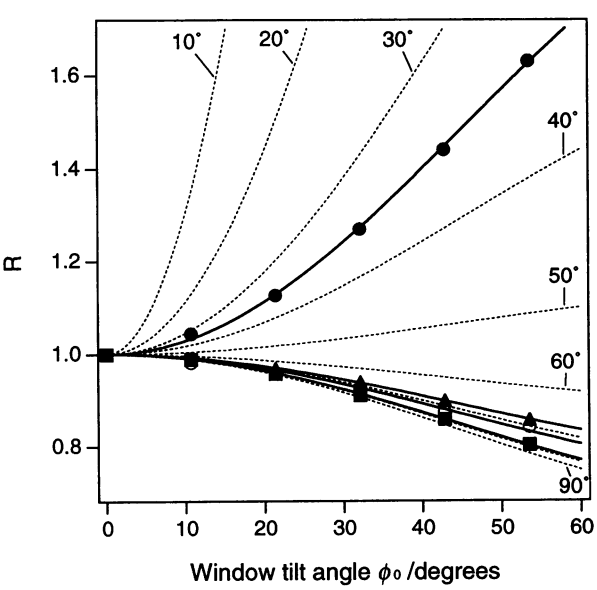

FIGURE 2 *R* versus ϕ_0 plots for the bands at 1761 cm^{-1} (●), 1527 cm^{-1} (○), 1202 cm^{-1} (■), and 1169 cm^{-1} (▲). The bands at 1527, 1202, and 1169 cm^{-1} are not included in Fig. 1. The points were fitted with Eq. 2 by the least-squares method. The fitted curves are shown by thick lines. Dotted lines show the theoretical lines according to Eq. 2 from θ_0 = 10–90°. The line at $\theta_0 = 10°$ has the largest slope. The slope decreases with the increment of the angle of θ_0 and becomes negative above 54.7° (magic angle).

bold lines through them), which are quite consistent with the corresponding values determined by Earnest et al. (1986), who used the ρ value of 0.95. If we had used lower ρ values, our data would show considerable deviations with increasing tilt angles from the theoretical curves. The present value of $\theta_0 = 36 \pm 1.0°$ for the C=O of Asp^{85} is different from 43° (Earnest et al., 1986), which was measured during the decay of the M intermediate at 250 K in films made from aqueous suspensions. Our value is rather close to 35 ± 5°, the value reported by Nabedryk and Breton (1986).

The M minus BR spectrum exhibits a bilobe of water O-H stretching vibrational bands at 3671 and 3643 cm^{-1}. The previous analysis of the L minus BR spectrum by use of D85N and D212N proteins has shown that the 3643-cm^{-1} band is due to a water molecule weakly H-bonding with Asp^{212} (Maeda et al., 1994; Kandori et al., 1995). This frequency is affected by substitution of amino acid residues in the extracellular domain, Tyr^{57}, Asp^{212}, Glu^{204}, Arg^{82}, and Asp^{85} in the presence of chloride (Fischer et al., 1994; Kandori et al., 1995; Brown et al., 1995a; Hatanaka et al., 1996; Chon et al., 1996). On the other hand, the 3671-cm^{-1} band in the M intermediate is not affected by these mutations, indicating that it refers to an O-H bond that is not near these residues. With increasing tilt angle of the window, intensities of the 3671- and 3643-cm^{-1} bands both decrease (Fig. 3), but the angle dependence of the decrease is larger for the 3671-cm^{-1} band than that of the 3643-cm^{-1} band. This indicates that the O-H bond in the M intermediate is oriented more perpendicularly to the membrane normal than in BR. The asymmetrical shapes of these bands suggest that there is a contribution from other bands located at lower frequencies. Increase in the tilt angle caused the shifts of the negative band from 3643 cm^{-1} to higher frequencies, whereas the peak of the band at 3671 cm^{-1} remained unchanged. This could result from the presence of a negative band at lower frequencies with responses to the tilt angle different from that of the main negative band. The differential of the M minus BR spectrum at $\phi_0 = 0°$ gave the peak position of the main bands at 3643 and 3671 cm^{-1}. The same spectrum was then fitted by convoluted bands of Gaussian and Lorentzian functions of these two bands together with an additional three bands with peaks at 3660 (+), 3632 (−), and 3621 (−) cm^{-1} (Fig. 4). The bilobe of 3660- and 3632-cm^{-1} bands is more intense in E204D at pH 7 but absent at pH 10 (Hatanaka et al., unpublished results). By keeping the same peak frequencies and the FWHM at 26 and 32 cm^{-1} for the 3671- and 3643-cm^{-1} bands, respectively, a series of the spectra recorded with different ϕ_o was divided in a similar procedure. The area under the peak was calculated for each 3671- and 3643-cm^{-1} band, and the plots of R versus ϕ_0 were fitted to Eq. 2. The best fits with the least-squares deviations were obtained with 60 ± 0.4° for the 3643-cm^{-1} band of the unphotolyzed state, and 87 ± 4.9° for the 3671-cm^{-1} band of the M intermediate (Fig. 5).

DISCUSSION

The O-H stretching frequency at 3643 cm^{-1} of the water molecule in the BR state shifts by several cm^{-1} toward lower frequencies when Tyr^{57} (Fischer et al., 1994), Asp^{212} (Kandori et al., 1995), Glu^{204} (Brown et al., 1995a), Arg^{82} (Hatanaka et al., 1996), and Asp^{85} (Chon et al., 1996), residues in the extracellular domain, are replaced. On the

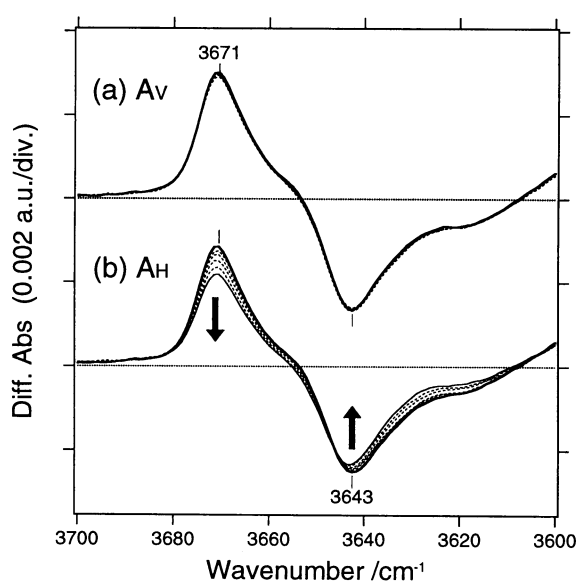

FIGURE 3 Changes of the M minus BR spectra in the 3700–3600 cm^{-1} region with the tilting of the sample window for the A_V (*a*) and A_H (*b*) components. The thick solid lines are the spectra at $\phi_0 = 0°$; the dotted lines are those at ϕ_0 = 10.7, 21.4, 32.1 and 42.8°; the thin solid line is that at $\phi_0 = 53.5°$. Arrows indicate the direction for the spectral changes with the tilting.

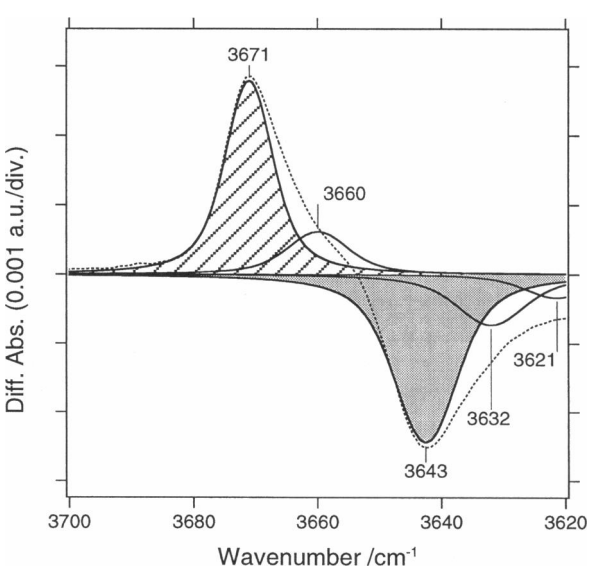

FIGURE 4 The decomposition of the difference spectrum of A_H at $\phi_0 = 0°$. The difference spectrum was decomposed to five components (*solid lines*) by assuming each band has convoluted spectral shape with Gaussian and Lorentzian functions. The dotted line represents the difference spectrum obtained by the experiments.

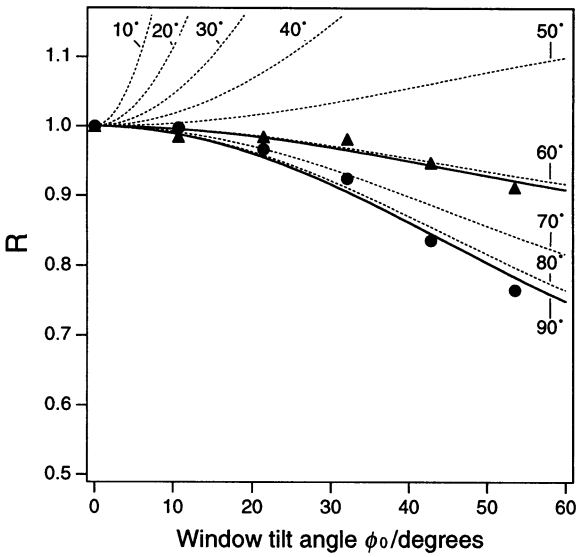

FIGURE 5 R versus ϕ_0 plot for the vibrational bands of water at 3671 cm^{-1} (●) and 3643 cm^{-1} (▲). The points were fitted with Eq. 2 by the least-squares method. The fitted curves were shown by thick lines. Dotted lines show the theoretical lines according to Eq. 2 from θ_0 = 10–90°. The line at θ_0 = 10° has the largest slope, and the slope decreases with the increment of the angle of θ_0.

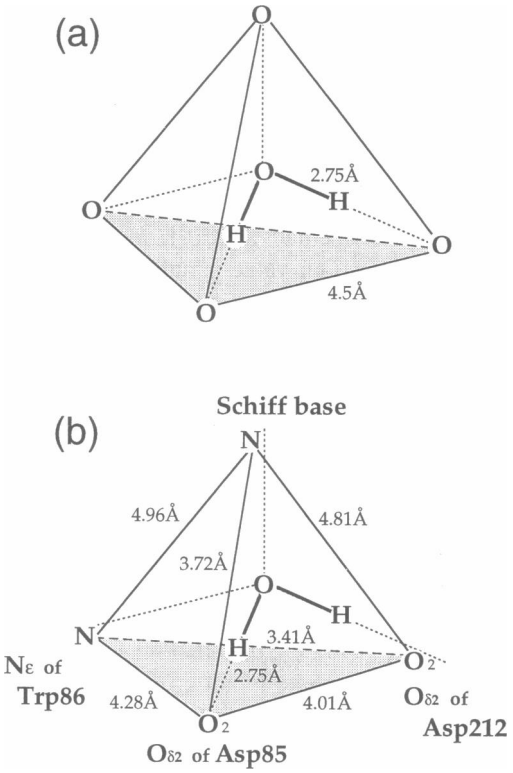

FIGURE 6 Comparison of tetrahedral ice (*a*) with the distorted tetrahedron with the nitrogen of the Schiff base, the N_ϵ of the indole of Trp^{86}, the $O_{\delta 2}$ of carboxylate of Asp^{85}, and the $O_{\delta 2}$ of carboxylate of Asp^{212} at the four apices (*b*). The oxygen of a water molecule (whose O-H bonds are represented by thick lines) is placed at the center of the real tetrahedron in both *a* and *b*. Dotted lines connect the center and four apexes of the real tetrahedron. The invisible bottom plane is represented by the dark area.

other hand, the O-H stretching vibration at 3671 cm^{-1} in the M intermediate is not affected at all by these mutations. Thus it is likely that the water molecule for the 3671-cm^{-1} band in the M intermediate is not located in the places influenced by these residues. The relation between these two bands, which form a nice bilobe, is an issue for future studies. The present results show that the O-H bond that is the origin of the 3671-cm^{-1} band in the M intermediate lies almost parallel to the membrane plane. Even though this functional water molecule is not covalently bound to the protein, it is located at a fixed position relative to the other O-H bond in the protein matrix.

The model from cryoelectron diffraction for the unphotolyzed state of bacteriorhodopsin (Grigorieff et al., 1996) shows cavities, with radii of >0.12 nm, which are able to accommodate a water molecule, to the extracellular side of Asp^{85} but not in the space between Asp^{85} and the Schiff base. Our FTIR spectroscopic studies, however, have shown the presence of a water molecule H-bonded to the Schiff base, Asp^{85}, Asp^{212} (Kandori et al., 1995; Chon et al., 1996), and Trp^{86} (Hatanaka et al., 1997). Such an internal water molecule must be placed in this site by forming an ice-like structure with four H-bonds. We can place the four suggested H-bonding partners of water, the N-H of the Schiff base, the C-$O_{\delta 2}$ of carboxylate of Asp^{212}, and the C-$O_{\delta 2}$ of carboxylate of Asp^{85}, along with the N_ϵ-H of the indole of Trp^{86}, within the coordinates by Grigorieff et al. (1996). They form four apexes of a distorted tetrahedron with the oxygen of water in the center (Fig. 6 *b*), although the distances between them deviate from those in the authentic tetrahedron of ice (Fig. 6 *a*). Because H-bonding with Asp^{85} must be strongest (Kandori et al., 1995), the oxygen of Asp^{85} is placed at one of the apexes. This is the most favorable position for forming strong H bonding (Thanki et al., 1988). In this way, however, the other atoms that form H bonds are not located at the apexes of the tetrahedron. This is reasonable because skewed geometries for all of the others will cause weaker H bonding. Weak H bonding of the Schiff base (de Groot et al., 1989) and Asp^{212} (Kandori et al., 1995) is known to occur. Trp^{86} mainly interacts with $O_{\delta 1}$ of Asp^{212} (Grigorieff et al., 1996) and therefore only weakly interacts with the water molecule, as shown by the abolition of the structural changes of water in W86F (Hatanaka et al., 1997). One can plant this distorted tetrahedron in the protein environment with a tilted orientation, as in Fig. 7. The angle between the O-H bond and the membrane normal is 60° in this alignment. This is in very good agreement with the value calculated from the experiments.

The same model (Grigorieff et al., 1996) shows that the C-$O_{\delta 1}$ bond of Asp^{85} forms an angle of 25.5° and the C-$O_{\delta 2}$ bond an angle of 71.2° to the membrane normal. The C-$O_{\delta 2}$ bond is located at a position favorable for accepting a proton from the Schiff base, and hence is assigned to the protonated carbonyl bond in the M intermediate. It is also at the right

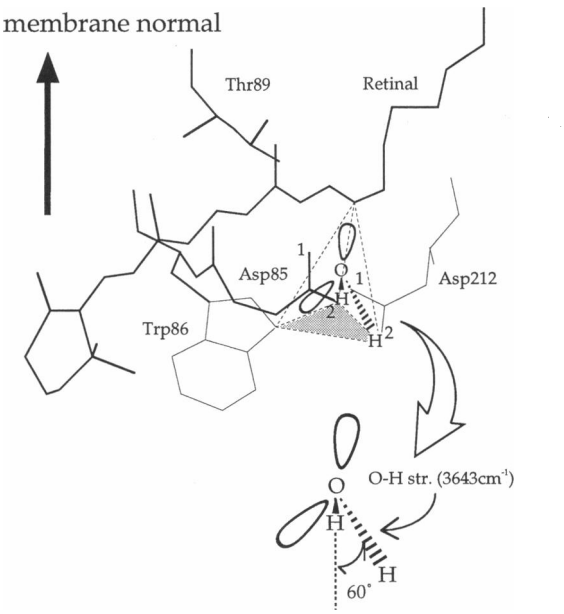

FIGURE 7 The alignment of the distorted tetrahedron of Fig. 6 *b* in the protein. The shaded bottom plane in Fig. 6 *b* faces toward the front of this figure. Labels 1 and 2 on the C-O bonds stand for $O_{\delta 1}$ and $O_{\delta 2}$. A dotted line in the expanded figure of water was drawn to show the angle of the O-H to the vertical line to the membrane (*arrow*).

position to form strong H bonding with the water O-H, which is different from the O-H bond with a stretching frequency at 3643 cm^{-1}. The C-$O_{\delta 1}$ forms an H bond with the $O_{\gamma 1}$ of Thr^{89} in the unphotolyzed state. It will be preserved in the unprotonated carbonyl state in the M intermediate. The measured angle of 36° for the C=O stretching vibration of the protonated Asp^{85} in the M intermediate is not markedly different from the value of 25.5° for BR from the diffraction study (Grigorieff et al., 1996), indicating only small structural changes in the BR-to-M process.

It is necessary to ascertain the energetic feasibility of accommodating this water molecule at this site, but this must be an issue for the future. Many lines of evidence, however, already strongly suggest the presence of the water molecule in this position. The presence of a water molecule next to the Schiff base was suggested from rapid H-D exchange of the Schiff base proton (Deng et al., 1994), energy transfer of the Schiff base vibration to a water molecule (Hildebrandt and Stockburger, 1984), a neutron diffraction study (Papadopoulos et al., 1990), and FTIR and FT-Raman studies on the frequency shifts of water and the Schiff base N-H (Chon et al., 1996). Molecular dynamic simulations (Zhou et al., 1993; Humphrey et al., 1994; Scharnagl et al., 1994; Roux et al., 1996) and ab initio quantum chemical calculations (Nina et al., 1995) on the basis of the 1990 structural model (Henderson et al., 1990) include water molecules between the Schiff base and Asp^{85}. For the new diffraction map, no refined calculations have been applied. Furthermore, the negatively charged carboxylates of Asp^{85} and Asp^{212} have not been well resolved (Grigorieff et al., 1996).

Environment change that decreases the dielectric constant around Asp^{85} occurs in the M intermediate, as reflected by a high frequency of its C=O stretching vibration at 1761 cm^{-1} (Dioumaev and Braiman, 1995). This is the cause of the large increase in the pK_a value of Asp^{85} in the BR-to-M conversion. Among the H-bonding partners of the water molecule in Fig. 7, Asp^{85} is protonated and the Schiff base loses the proton in the M intermediate. These changes in structure then cause the release of the water molecule from the site of Asp^{85} and abolish H bonding with Thr^{89}. These may suffice for the decreased dielectric environment. Molecular dynamic calculations also show that Asp^{85} is not interacting with water molecules in the M intermediate (Xu et al., 1995). In the low dielectric protein environment, the charges of the protonated Schiff base and carboxylate would tend to cancel each other. Dielectric coupling to stabilize the ionic pair (Scheiner and Duan, 1991) could be achieved only by an intervening water molecule, as shown in Fig. 7. Once this structure collapses upon isomerization, the water molecule cannot be kept, and the proton of the Schiff base moves to Asp^{85}. In other words, the structure proposed in Fig. 7 is a prerequisite for preventing the neutralization of the charged pair.

We thank Janos K. Lanyi for improving the style of the manuscript.

This work was partly supported by the grant from the Japanese Ministry of Education, Culture, Sport and Science to AM (06404082, 08268225) and HK (09833002, 09235213). MH is a recipient of a postdoctoral fellowship from the Japan Society for the Promotion of Science.

REFERENCES

Balashov, S. P., R. Govindjee, and T. G. Ebrey. 1991. Red shift of the purple membrane absorption band and the deprotonation of tyrosine residues at high pH. *Biophys. J.* 60:475–490.

Braiman, M. S., T. Mogi, T. Marti, L. S. Stern, H. G. Khorana, and K. J. Rothschild. 1988. Vibrational spectroscopy of bacteriorhodopsin mutants: light-driven proton transport involves protonation changes of aspartic acid residues 85, 96, and 212. *Biochemistry.* 27:8516–8520.

Brown, L. S., J. Sasaki, H. Kandori, A. Maeda, R. Needleman, and J. K. Lanyi. 1995a. Glutamic acid 204 is the terminal proton release group at the extracellular surface of bacteriorhodopsin. *J. Biol. Chem.* 270: 27122–27126.

Brown, L. S., G. Váró, M. Hatanaka, J. Sasaki, H. Kandori, A. Maeda, N. Friedman, M. Sheves, R. Needleman, and J. K. Lanyi. 1995b. The complex extracellular domain regulates the deprotonation and reprotonation of the retinal Schiff base during the bacteriorhodopsin photocycle. *Biochemistry.* 34:12903–12911.

Chon, Y.-S., J. Sasaki, H. Kandori, L. S. Brown, J. K. Lanyi, R. Needleman, and A. Maeda. 1996. Hydration of the counterion of the Schiff base in the chloride-transporting mutant of bacteriorhodopsin: FTIR and FT-Raman studies on the effects of anion binding when Asp^{85} is replaced with a neutral residue. *Biochemistry.* 35:14244–14250.

de Groot, H. J. M., G. S. Harbison, J. Herzfeld, and R. G. Griffin. 1989. Nuclear magnetic resonance study of the Schiff base in bacteriorhodopsin: counterion effects on the ^{15}N shift anisotropy. *Biochemistry.* 28:3346–3353.

Deng, H., L. Huang, R. Callender, and T. Ebrey. 1994. Evidence for a bound water molecule next to the retinal Schiff base in bacteriorhodop-

sin and rhodopsin: a resonance Raman study of the Schiff base hydrogen-deuterium exchange. *Biophys. J.* 66:1129–1136.

Dioumaev, A. K., and M. S. Braiman. 1995. Modeling vibrational spectra of amino acid side chains in proteins: the carbonyl stretch frequency of buried carboxylic residues. *J. Am. Chem. Soc.* 117:10572–10574.

Earnest, T. N., P. Roepe, M. S. Braiman, J. Gillespie, and K. J. Rothschild. 1986. Orientation of the bacteriorhodopsin chromophore probed by polarized Fourier transform infrared difference spectroscopy. *Biochemistry.* 25:7793–7798.

Fahmy, K., F. Siebert, M. F. Grossjean, and P. Tavan. 1989. Photoisomerization in bacteriorhodopsin studied by FTIR, linear dichroism and photoselection experiments combined with quantum chemical theoretical analysis. *J. Mol. Struct.* 214:257–288.

Fischer, W. B., S. Sonar, T. Marti, H. G. Khorana, and K. J. Rothschild. 1994. Detection of a water molecule in the active-site of bacteriorhodopsin: hydrogen bonding changes during the primary photoreaction. *Biochemistry.* 33:12757–12762.

Grigorieff, N., T. A. Ceska, K. H. Downing, J. M. Baldwin, and R. Henderson. 1996. Electron-crystallographic refinement of the structure of bacteriorhodopsin. *J. Mol. Biol.* 259:393–421.

Hatanaka, M., R. Kashima, H. Kandori, N. Friedman, M. Sheves, R. Needleman, J. K. Lanyi, and A. Maeda. 1997. Trp86 → Phe replacement in bacteriorhodopsin affects a water molecule near Asp85 and light adaptation. *Biochemistry.* 36:5493–5498.

Hatanaka, M., J. Sasaki, H. Kandori, T. G. Ebrey, R. Needleman, J. K. Lanyi, and A. Maeda. 1996. Effects of arginine-82 on the interactions of internal water molecules in bacteriorhodopsin. *Biochemistry.* 35: 6308–6312.

Henderson, R., J. M. Baldwin, T. A. Ceska, F. Zemlin, E. Beckman, and K. H. Downing. 1990. Model for the structure of bacteriorhodopsin based on high-resolution electron cryomicroscopy. *J. Mol. Biol.* 213:899–929.

Hildebrandt, P., and M. Stockburger. 1984. Role of water in bacteriorhodopsin's chromophore: resonance Raman study. *Biochemistry.* 23: 5539–5548.

Humphrey, W., I. Logunov, K. Schulten, and M. Sheves. 1994. Molecular dynamics study of bacteriorhodopsin and artificial pigments. *Biochemistry.* 33:3668–3678.

Kandori, H., Y. Yamazaki, J. Sasaki, R. Needleman, J. K. Lanyi, and A. Maeda. 1995. Water-mediated proton transfer in proteins: an FTIR study of bacteriorhodopsin. *J. Am. Chem. Soc.* 117:1713–1714.

Lanyi, J. K. 1993. Proton translocation mechanism and energetics in the light-driven pump bacteriorhodopsin. *Biochim. Biophys. Acta.* 1183: 241–261.

Maeda, A., H. Kandori, Y. Yamazaki, S. Nishimura, M. Hatanaka, Y. -S. Chon, J. Sasaki, R. Needleman, and J. K. Lanyi. 1997. Intramembrane signaling mediated by hydrogen-bonding of water and carboxyl groups in bacteriorhodopsin and rhodopsin. *J. Biochem.* 121:399–406.

Maeda, A., J. Sasaki, Y. Shichida, and T. Yoshizawa. 1992. Water structural changes in the bacteriorhodopsin photocycle: analysis by Fourier transform infrared spectroscopy. *Biochemistry.* 31:462–467.

Maeda, A., J. Sasaki, Y. Yamazaki, R. Needleman, and J. K. Lanyi. 1994. Interaction of aspartate-85 with a water molecule and the protonated Schiff base in the L intermediate of bacteriorhodopsin: a Fourier transform infrared spectroscopic study. *Biochemistry.* 33:1713–1717.

Nabedryk, E., and J. Breton. 1986. Polarized Fourier transform infrared (FTIR) difference spectroscopy of the M_{412} intermediate in the bacteriorhodopsin photocycle. *FEBS Lett.* 202:356–360.

Nina, M., B. Roux, and J. C. Smith. 1995. Functional interactions in bacteriorhodopsin: a theoretical analysis of retinal hydrogen bonding with water. *Biophys. J.* 68:25–39.

Oesterhelt, D., and W. Stoeckenius. 1974. Isolation of the cell membrane of *Halobacterium halobium* and its fractionation into red and purple membrane. *Methods Enzymol.* 31:667–678.

Papadopoulos, G., N. A. Dencher, G. Zaccai, and G. Büldt. 1990. Water molecules and exchangeable hydrogen ions at the active center of bacteriorhodopsin localized by neutron diffraction. Elements of the proton pathway? *J. Mol. Biol.* 214:15–19.

Rothschild, K. J., and N. A. Clark. 1979. Polarized infrared spectroscopy of oriented purple membrane. *Biophys. J.* 25:473–488.

Roux, B., M. Nina, R. Pomès, and J. C. Smith. 1996. Thermodynamic stability of water molecules in the bacteriorhodopsin proton channel: a molecular dynamics free energy perturbation study. *Biophys. J.* 71: 670–681.

Scharnagl, C., J. Hettenkofer, and S. F. Fischer. 1994. Proton release pathway in bacteriorhodopsin: molecular dynamics and electrostatic calculations. *Int. J. Quant. Chem. Quant. Biol. Symp.* 21:33–56.

Scheiner, S., and X. Duan. 1991. Effects of intermolecular orientation on proton transfer within a polarizable medium. *Biophys. J.* 60:874–883.

Thanki, N., J. M. Thornton, and J. M. Goodfellow. 1988. Distribution of water around amino acid residues in proteins. *J. Mol. Biol.* 202: 637–657.

Xu, D., M. Sheves, and K. Schulten. 1995. Molecular dynamics study on the M_{412} intermediate of bacteriorhodopsin. *Biophys. J.* 69:2745–2760.

Zhou, F., A. Windemuth, and K. Schulten. 1993. Molecular dynamics study of the proton pump cycle of bacteriorhodopsin. *Biochemistry.* 32:2291–2306.